

Reactive nanostructured foil used as a heat source for joining titanium

A. Duckham, S. J. Spey, J. Wang, M. E. Reiss, T. P. Weihs, E. Besnoin, and O. M. Knio

Citation: *Journal of Applied Physics* **96**, 2336 (2004); doi: 10.1063/1.1769097

View online: <https://doi.org/10.1063/1.1769097>

View Table of Contents: <http://aip.scitation.org/toc/jap/96/4>

Published by the [American Institute of Physics](#)

Articles you may be interested in

[Joining of stainless-steel specimens with nanostructured Al/Ni foils](#)

Journal of Applied Physics **95**, 248 (2004); 10.1063/1.1629390

[Room-temperature soldering with nanostructured foils](#)

Applied Physics Letters **83**, 3987 (2003); 10.1063/1.1623943

[Effect of reactant and product melting on self-propagating reactions in multilayer foils](#)

Journal of Applied Physics **92**, 5474 (2002); 10.1063/1.1509840

[Protein labeling reactions in electrochemical microchannel flow: Numerical simulation and uncertainty propagation](#)


Physics of Fluids **15**, 2238 (2003); 10.1063/1.1582857

[Characteristics of coherent vortical structures in turbulent flows over progressive surface waves](#)

Physics of Fluids **21**, 125106 (2009); 10.1063/1.3275851

[Investigation of coupled air-water turbulent boundary layers using direct numerical simulations](#)


Physics of Fluids **21**, 062108 (2009); 10.1063/1.3156013



Instruments for Advanced Science


Contact Hiden Analytical for further details:
W www.HidenAnalytical.com
E info@hiden.co.uk

[CLICK TO VIEW](#) our product catalogue



Gas Analysis

- dynamic measurement of reaction gas streams
- catalysis and thermal analysis
- molecular beam studies
- dissolved species probes
- fermentation, environmental and ecological studies




Surface Science

- UHV TPD
- SIMS
- end point detection in ion beam etch
- elemental imaging - surface mapping



Plasma Diagnostics

- plasma source characterization
- etch and deposition process reaction kinetic studies
- analysis of neutral and radical species



Vacuum Analysis

- partial pressure measurement and control of process gases
- reactive sputter process control
- vacuum diagnostics
- vacuum coating process monitoring

Reactive nanostructured foil used as a heat source for joining titanium

A. Duckham,^{a)} S. J. Spey, J. Wang, M. E. Reiss, and T. P. Weihs
*Department of Materials Science and Engineering, The Johns Hopkins University,
Baltimore, Maryland 21218*

E. Besnoin and O. M. Knio
Department of Mechanical Engineering, The Johns Hopkins University, Baltimore, Maryland 21218

(Received 20 October 2003; accepted 17 May 2004)

We have joined titanium alloy (Ti-6Al-4V) specimens at room temperature and in air by using free-standing nanostructured Al/Ni multilayer foils to melt a silver-based braze. The foils are capable of undergoing self-sustaining exothermic reactions and thus act as controllable local heat sources. By systematically controlling the properties of the foils and by numerically modeling the reactive joining process, we are able to conclude that the temperatures reached by the foils during reaction are critical in determining the success of joining when using higher melting temperature braze layers. © 2004 American Institute of Physics. [DOI: 10.1063/1.1769097]

I. INTRODUCTION

The use of nanostructured reactive multilayered foils as a heat source represents an exciting addition to the field of joining.^{1–7} The energy released by self-propagating exothermic reactions in reactive multilayered foils can be harnessed to melt bonding layers (solders or brazes) to join components. This technique, known as reactive joining, has a number of significant advantages compared to more conventional soldering and brazing techniques: no external heat sources (except to trigger the reaction) are required; joining can be performed in any atmosphere or under vacuum; and the temperatures of the joined components are never raised significantly. Therefore temperature sensitive components are not compromised and large components with very different coefficients of thermal expansion can be joined.

Previous studies have demonstrated the ability to measure, model, and therefore control properties such as the reaction velocity, reaction heat, temperature evolution, and phase formation during self-propagating reactions in multilayer systems.^{8–17} This knowledge has enabled more recent efforts to optimize the reactive joining of components made from various materials, using different bonding layers. For example, Au coated stainless steel joints using AuSn solder and reactive foils have been shown to be 25% stronger compared with conventional AuSn solder joints;³ and bulk metallic glass has been welded using reactive foils without causing crystallization of the glass components.⁶

In this study we focus on the reactive joining of a commercial titanium alloy using reactive Al/Ni multilayer foils and a bonding layer that has a high melting temperature, T_m (a silver based braze). It is expected that the reactive joining process will become more challenging as the melting point of the bonding layers increase. The question arises, will the rapid formation reaction of the foil, which causes the temperature of the foil to increase and decrease rapidly, transfer enough heat at a sufficient rate from the reactive foil into the bonding layers to enable melting.

II. EXPERIMENTAL METHOD

Freestanding Al/Ni multilayer foils were fabricated using magnetron sputtering, by rotating a water-cooled brass substrate over fixed Al and Ni guns. The Al target material was the commercial aluminum alloy, 1100, which has a minimum purity of 99 wt %. The Ni target was a nonmagnetic Ni-7V alloy. The ratio of the Al to the Ni layer thickness was adjusted to produce a 1:1 atomic ratio of Al to Ni-V. Two different sputtering runs were used to fabricate foils for this study. One run produced foils that contained 2000 bilayers with a range in bilayer dimension of 25–80 nm and a range in foil thickness of 50–160 μm . The other run produced foils that contained 4273 bilayers with the same range of bilayer period, but with a foil thickness range of 107–340 μm . The deposition process also included depositing a thin, 1 μm layer of Incusil-ABA braze (Ag-27.3Cu-12.5In-1.25Ti supplied by Wesgo Metals) on either side of the Al/Ni multilayer without breaking vacuum. This was done to enhance wetting during the joining process. Following deposition, the coated multilayer was peeled off the brass substrate so that it was freestanding.

The Al/Ni multilayer foils were characterized in various ways. As-deposited and reacted foils were examined by x-ray diffraction to determine phase formation. The heats of reaction were calculated by integrating net heat flow measured by differential scanning calorimetry (DSC) at a heating rate of 40 °C/min. The velocities of reaction in the foils were also measured using an optical system that records the intensity of light from the reaction as it passes through a mask with slits at a known periodic spacing, as described previously.¹⁸ These measurements were later used as inputs to numerically predict thermal transport during the joining process.

The freestanding Al/Ni reactive multilayer foils were used to join pieces of commercial Ti-6Al-4V alloy. Rectangular pieces of Ti-6Al-4V (20 × 10 mm²) were sectioned from a 0.41 mm thick sheet. They were prebrazed with Incusil-ABA by a conventional method of silk screening the braze in paste form, oven drying, and a heat treatment in

^{a)}Author to whom correspondence should be addressed.

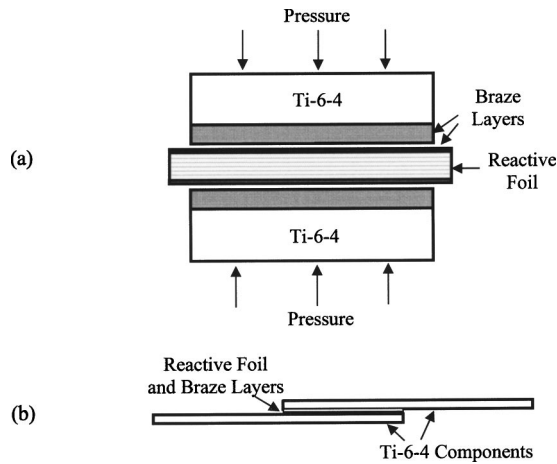


FIG. 1. Schematic diagrams showing the geometry of the reactive joining process: (a) transverse cross-sectional view, (b) longitudinal cross-sectional view of shear lap specimen.

vacuum near the T_m of the braze (at $710\text{ }^\circ\text{C}$). The prebrazed layers of Incusil-ABA were ground down to a thickness of $25\text{--}30\text{ }\mu\text{m}$. These pieces of prebrazed Ti-6Al-4V were sandwiched around a Al/Ni reactive foil with outer layers of Incusil-ABA [Fig. 1(a)]. A pressure of 35 Mpa was applied to the assembly and the multilayered reactive foil was then ignited with a spark. Heat released from the self-propagating formation reaction of the foil caused the braze layers on the foil and titanium pieces to melt, wet each other, and then solidify, thereby effecting a joint. It is important to note that this joining was performed in air and at room temperature.

The strengths of the joints produced were evaluated by tensile testing the resulting shear lap specimens [Fig. 1(b)] at room temperature. Shear strengths were calculated by dividing the maximum load at failure by the joint area ($10 \times 8\text{ mm}^2$). Fracture surfaces were examined by optical and scanning electron microscopy (SEM) to assess failure modes and the degree of wetting that occurred during joining. The integrities of the joints prior to testing were evaluated by performing cross-sectional optical and SEM microscopy, including compositional analysis by energy dispersive spectroscopy (EDS).

Heat transfer during the joining process was numerically modeled. The amount of braze on the titanium components that melted as well as the duration of melting was predicted. The model (described in more detail in Ref. 3) is composed of a simplified description of the self-propagating reaction linked with thermal transport and phase evolution in the braze layers and titanium components. The model assumes one-dimensional motion of the reaction front, which is described using the experimentally determined heats and velocities of reaction. Our computation focuses on simulating heat flow into the braze layers and phase changes within these layers. The temperature evolution can be obtained by integration of the energy conservation equation, which is independently solved within the reactive foil, braze layers, and titanium components

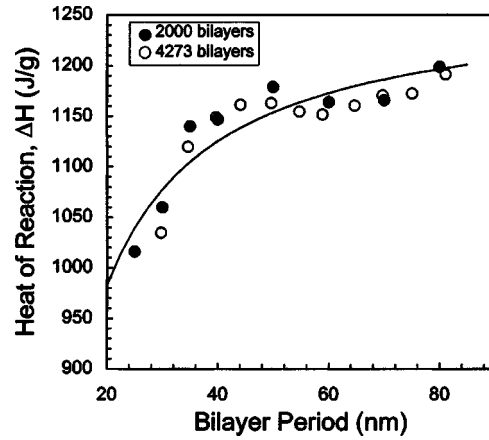


FIG. 2. Heats of reaction measured using DSC for the two sets of Al/Ni reactive foils plotted as a function of bilayer period: Scans could only be conducted to $600\text{ }^\circ\text{C}$ for the 4273 bilayer foils, so these values were systematically extrapolated from 600 to $725\text{ }^\circ\text{C}$ using data from the 2000 bilayer foils, for which scans were conducted to $725\text{ }^\circ\text{C}$. The plotted line is fitted to the data of the foils with 2000 bilayers according to Eq. (2).

$$\rho \frac{\partial h}{\partial t} = \nabla \cdot q + \dot{Q}, \tag{1}$$

where ρ and h are the density and enthalpy of the corresponding layer, t is time, q is the heat flux vector, and \dot{Q} is the heat release rate. The temperature T is related to enthalpy h by a relationship that involves that particular layer's heat capacity c_p and latent heat h_f . Note that \dot{Q} is nonzero in the reactive foil layer only, and is furthermore localized within the moving propagation front. A third-order finite-difference discretization of the energy equation is used in conjunction with explicit third-order time integration of the discretized evolution equations. The boundary conditions for the temperatures in each layer are determined by a thermal interface model, which accounts for thermal resistance at the interfaces between unbonded layers and which is assumed to decrease exponentially when melting and wetting occurs.

III. RESULTS

A. Characterization of reactive foils

The heat of reaction ΔH which is a specific quantity and is measured in Joule/gram was determined for the Al/Ni multilayer foils by integrating differential scanning calorimetry (DSC) curves. For the 2000 bilayer sputtering run some of the foil was not coated with braze, so direct measurements of heats of reaction up to $725\text{ }^\circ\text{C}$ were possible. For the 4273 bilayer sputtering run, however, all of the foil was coated with braze, so DSC scans were conducted up to $600\text{ }^\circ\text{C}$ (below the melting point of the braze). The heats of reaction as a function of bilayer were very similar for the two sputtering runs when measured up to $600\text{ }^\circ\text{C}$. The heats of reaction up to $725\text{ }^\circ\text{C}$ for the 4273 bilayer sputtering run, were then extrapolated by evaluating the heat of reaction between 600 and $725\text{ }^\circ\text{C}$ for the 2000 bilayer run and adding this quantity to that already measured for the 4273 bilayer run up to $600\text{ }^\circ\text{C}$. This was all done as a function of bilayer. The results are plotted as a function of bilayer period, λ , in Fig. 2.

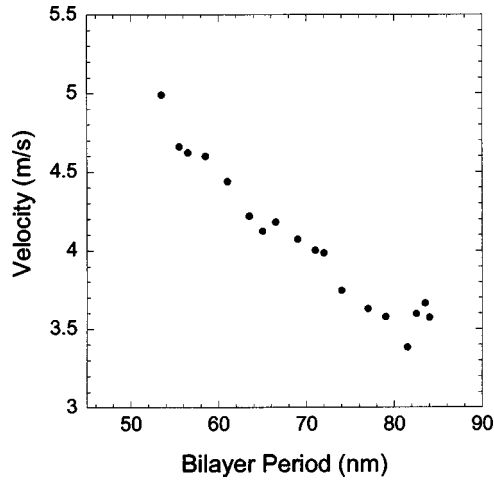


FIG. 3. Velocity of self-propagating reactions in the Al/Ni reactive foils that consist of 2000 bilayers.

The heat of reaction is seen to increase as the bilayer period increases, and the trend is very similar for both sputtering runs. There is about a 20% difference in values over the bilayer range investigated: from 1000 J/g for a 20 nm bilayer thickness to 1200 J/g for a 80 nm bilayer thickness. The reason for this dependence of the heat of reaction on bilayer period is due to the inevitable intermixing of the layers that occurs during deposition, and which causes a reduction in the maximum possible amount of heat that can be released, ΔH_0 .¹¹ The absolute amount of intermixing is usually constant for a given deposition, and is defined by an intermixed layer of thickness w . The measured heat of reaction ΔH however, is dependent on the fractional amount of intermixing, w/λ , and can be expressed as

$$\Delta H = \Delta H_0 \left(1 - \frac{2w}{\lambda} \right). \quad (2)$$

The data for the sputtering run that produced 2000 bilayers that is shown in Fig. 2 had previously been plotted versus $1/\lambda$ and a linear fit indicated that the intermixed layer w was 2.3 ± 0.3 nm and that ΔH_0 was 1270 ± 20 J/g.³ Using these values of w and ΔH_0 , heats of reaction were calculated according to Eq. (2) for the whole bilayer range investigated and these are shown by the solid line in Fig. 2. These calculated heats of reaction were used as inputs for the numerical modeling.

Reaction velocities were measured as a function of bilayer period and the results are plotted in Fig. 3. Velocities are seen to increase as bilayer period decreases since diffusion distances become smaller and atoms can mix more rapidly. Heat is thus released at a higher rate and reactions travel faster through the reactive foil. The measured velocities range between 3.4 and 5 m s⁻¹.

X-ray diffraction on the as-deposited reactive foil revealed that all the major diffraction peaks corresponded to Al and Ni. After reaction in air, all major peaks corresponded to the AlNi compound.³ These results indicate that the thickness ratio of Al to Ni for the deposited reactive foils was very close to the ideal ratio to maximize the heat of reaction for the formation of AlNi.

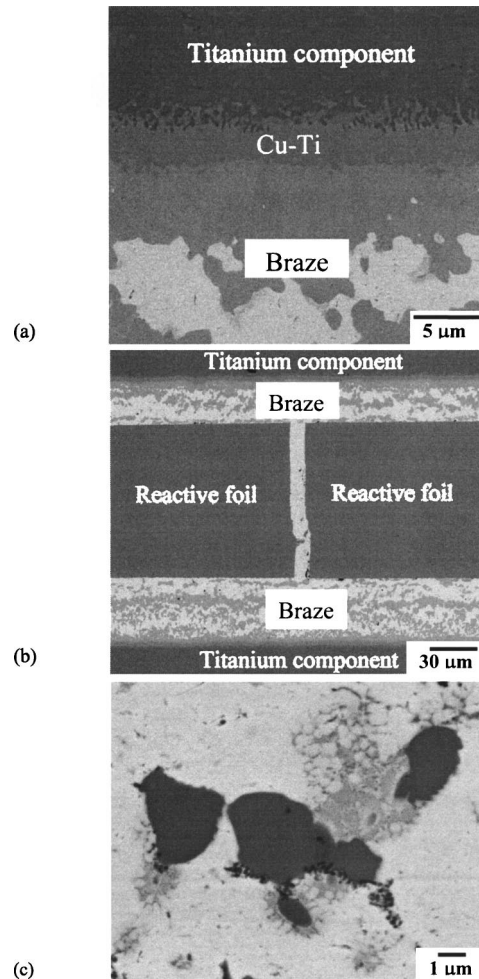


FIG. 4. Cross-sectional SEM micrographs of (a) braze on titanium component following pre-brazing but prior to joining: the braze contains two phases and a CuTi layer is observed to form between the braze and the titanium, (b) reactively joined titanium components: good adherence at all interfaces and braze flow into cracks in the reactive foil, and (c) melted regions of the braze following joining where refined microstructure is evident.

B. Characterization of joints

Cross-sections of prebrazed titanium alloy component pieces were initially examined prior to joining. An important observation is that an interface layer between the braze layer and the titanium component forms during the prebrazing process. This layer is clearly visible in Fig. 4(a) and semiquantitative EDS analysis of this layer indicates that it is a roughly equiatomic CuTi phase ($\text{Cu}_{48}\text{Ti}_{45}\text{Al}_5\text{Ag}_1\text{V}_{0.7}\text{In}_{0.3}$). It is also quite apparent from Fig. 4(a) that the braze consists of two chemically distinct phases. EDS analysis indicates that the lighter phase is Ag rich ($\text{Ag}_{82}\text{In}_{10}\text{Cu}_{7.5}\text{Ti}_{0.5}$), while the darker phase is Cu rich ($\text{Cu}_{57}\text{Ti}_{25}\text{In}_{12}\text{Al}_4\text{Ag}_2$). The average composition of the braze layer after prebrazing was also measured. It was found to contain a significantly higher amount of Ti compared to the supplied material (7 wt % compared to 1.25 wt %). Using a combination of DSC and differential thermal analysis the liquids temperature of this prebrazed layer was determined to be 805 °C. This is significantly higher than that of the supplied material, which is quoted to be 715 °C.

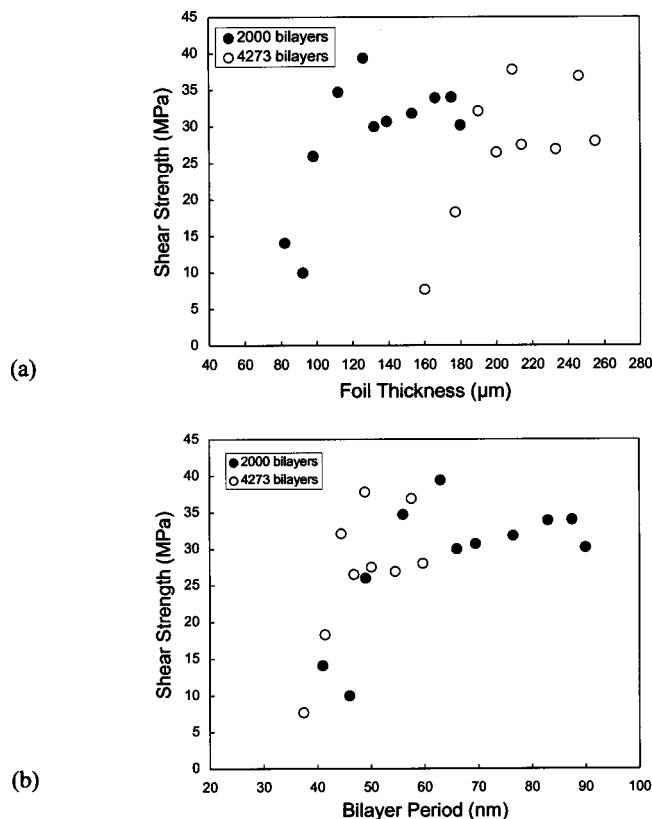


FIG. 5. Tensile shear strengths of shear lap specimens plotted as a function of: (a) the thickness of the Al/Ni reactive foils, (b) the bilayer period of the Al/Ni reactive foils.

Shear lap joints were made according to the geometry indicated in Fig. 1. Some of these joints were cross-sectioned for microscopy before any testing was conducted. Figure 4(b) shows a backscattered electron SEM micrograph of such a cross-sectioned joint and it is apparent that there is good wetting and adherence between all interfaces. In particular, the interface between the braze layer deposited on the foil and braze layer deposited on the titanium component is virtually undetectable. Also shown in Fig. 4(b) is a crack in the reactive foil that occurred and was filled with braze material during the joining process. This is typical of the larger cracks in the reactive foil that essentially form braze bridges linking the braze layers on either side of the reactive foil, and thereby form a composite adhesion layer between the titanium components. There is also good evidence of melting of the braze. Following joining the braze microstructure appears to be highly refined locally, with areas of an extremely fine lamellar eutectic structure visible [Fig. 4(c)]. The melting appears to be mostly confined to the Ag-rich phase of the braze, which presumably has the lower melting point of the two phases present in the braze. Also, melting is not always evident all the way through the $\sim 30 \mu\text{m}$ thickness of the braze layer that was prebrazed on the titanium component, even for maximum strength joints. The refined microstructure, which has been observed in a previous study on reactive joining,³ is due to the very rapid cooling following melting and is thought to be unique to the reactive joining process.

The tensile shear strengths of the reactively joined titanium alloy specimens are plotted in Fig. 5. In Fig. 5(a) the

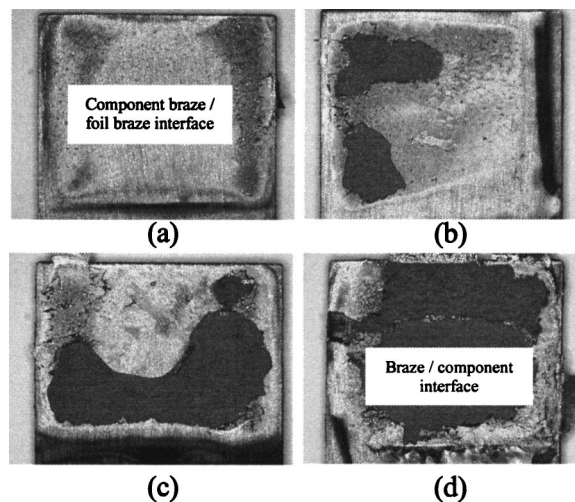


FIG. 6. Fracture surfaces after tensile shear tests of joints made using reactive foils containing 2000 bilayers: (a) only a small area of the braze on the titanium component appears to have melted and failure occurs exclusively along the component braze/foil braze interface (foil thickness = $92 \mu\text{m}$, joint strength = 10 MPa); (b) failure also starts to occur along the braze/component interface shown by the darker area (foil thickness = $98 \mu\text{m}$, joint strength = 26 MPa); (c) failure along the braze/component interface becomes more significant (foil thickness = $112 \mu\text{m}$, joint strength = 35 MPa); and (d) failure is now almost exclusively along the braze/component interface (foil thickness = $126 \mu\text{m}$, joint strength = 39 MPa).

results are plotted as a function of reactive foil thickness while in Fig. 5(b) they are plotted as a function of reactive foil bilayer period. In Fig. 5(a) it can be observed that shear strengths initially increase with foil thickness before leveling off to a value of about 33 MPa. Furthermore, this leveling off with foil thickness occurs at different foil thicknesses for the two foil sets investigated. It occurs at about $110 \mu\text{m}$ for the foil set with 2000 bilayers and at about $190 \mu\text{m}$ for the foil set with 4273 bilayers. Thus it would appear that joint strength, which is a good indicator of the success of joining, does not depend critically on the total foil thickness. Rather, it would appear that successful joining in this case depends critically on bilayer period as can be seen in Fig. 5(b), where the results for both foil sets show a similar dependency. Joint strength is observed to increase sharply as the bilayer period increases to about 50 nm, after which joint strength seems to reach a limiting value for higher values of bilayer period. A few joints were also made using Ti-6Al-4V blocks (10 mm thick) instead of the sheet, which enabled shear testing in compression instead of tension. Shear strengths of up to 102 MPa were thus measured. This demonstrated that the tensile mode of testing resulted in measurements that were far below the true shear strengths of the joints due to the additional nonshear loads imposed on the tensile single lap shear specimens.

The fracture surfaces of tested shear lap specimens were examined by optical stereo microscopy and SEM. For specimens that recorded very low shear strengths, fracture occurred almost exclusively along the component braze/foil braze interface and it was apparent that only a small amount of the braze on the component had melted [see Fig. 6(a)]. For higher recorded shear strengths, it was noticed that fracture also started to occur along the braze/component [Figs. 6(a)

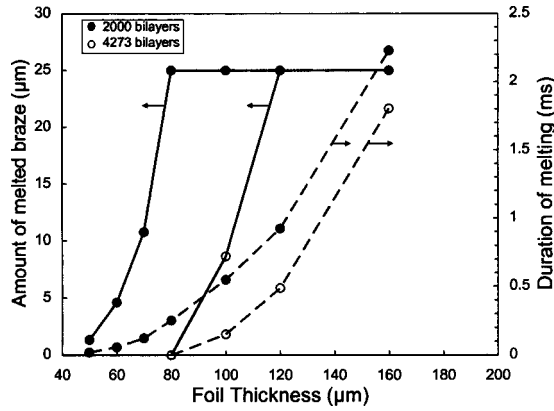


FIG. 7. Numerical predictions of the amount of melting (thickness of melted region as measured from the reactive foil interface) of the 25 μm predeposited braze layer on the titanium components (solid lines). The duration of melting at the component braze/foil braze interface is also plotted (dashed lines).

and 6(b)]. In fact, the increase in strength was found to be proportional to the fraction of failure along the braze/component interface. For the maximum recorded shear strength, failure was observed to occur almost exclusively along the braze/component interface [Fig. 6(d)]. SEM EDS analysis of the fracture surfaces revealed that when fracture did occur along the braze/component interface it was localized in or along the CuTi interface layer previously identified by cross-sectional SEM [Fig. 4(a)].

C. Numerical modeling results

The measured velocities and heats of reaction were fed into the numerical model for particular foil thicknesses and bilayer periods in order to replicate the experimental joining as closely as possible. The model output predicted the amount and time of melting for the braze layers. In Fig. 7 these outputs are plotted as a function of foil thickness for inputs that characterize the properties of the two different sets of foil. In a general sense this plot mimics the experimental shear strength values shown in Fig. 5(a). The predicted amount of melting of the braze layer on the titanium is seen to initially increase rapidly with foil thickness until it is all melted just as the shear strengths are observed to increase rapidly before leveling off. Furthermore, the predictions in Fig. 7 for the two different foil sets clearly show different dependencies on foil thickness, as was the case for the measured shear strengths in Fig. 5(a), although the separation of the data is not as pronounced in Fig. 7 compared to Fig. 5(a). The predicted duration of melting of the braze layer on the component measured at the interface with the thin braze layer on the foil is also shown in Fig. 7. This duration of melting shows a steady increase as foil thickness increases for both sets of foil. From the experimental data in Fig. 5(a) it was observed that the measured shear strengths level off at a foil thickness of 110 μm for the foil set consisting of 2000 bilayers. The predicted duration of melting for this same foil set at 110 μm is about 0.75 ms (from Fig. 7). The implication therefore is that the braze on the component needs to be molten for at least 0.75 ms at the unbonded interface to achieve maximum wetting and joint strength.

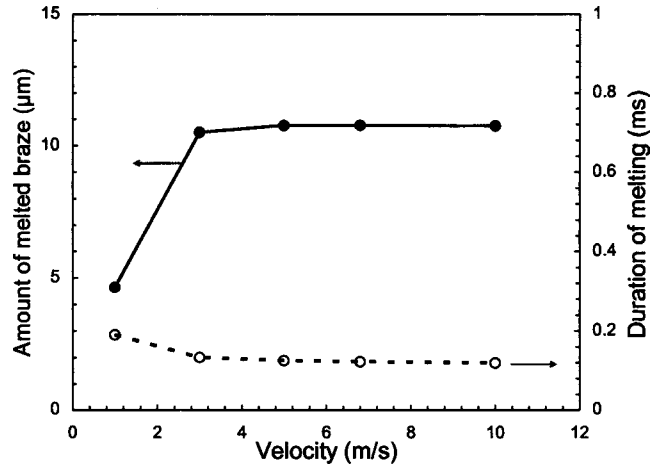


FIG. 8. Numerical parametric study which reflects the dependence of melting of the 25 μm predeposited braze layer on the velocity of reaction in the Al/Ni reactive foil. The foil heat of reaction ΔH and the foil thickness were kept constant at 1126 J/g and 70 μm, respectively.

Numerical parametric studies were also conducted in order to isolate the effects of the velocity of reaction, the heat of reaction, and the total reaction heat on the melting of the braze layers. Figure 8 shows the effect of changing only the velocity of reaction while keeping all other parameters constant. For velocities of 3 m/s and higher, it is predicted that velocity has very little effect on both the amount and duration of melting. The lowest experimentally measured velocity for all the reactive foils investigated was 3.4 m/s (Fig. 3), so for this study it is expected that velocity of reaction has little or no influence on results.

The effect of varying the total heat released from the reactive foil was modeled by changing the foil thickness only, while keeping the heat of reaction constant at 1000 J/g and velocity constant at 5 m/s. These results are plotted in Fig. 9, where it can be seen that the foil thickness (and therefore also the total heat) needs to be doubled (from 60 to 120

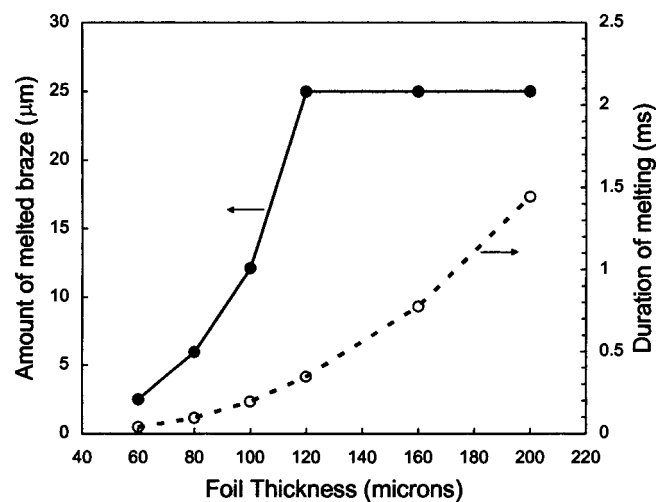


FIG. 9. Numerical parametric study which reflects the dependence of melting of the 25 μm predeposited braze layer on the total heat released by the Al/Ni reactive foil. The total heat was varied by increasing the foil thickness while keeping the heat of reaction ΔH and the velocity constant at 1000 J/g and 5 m/s, respectively.

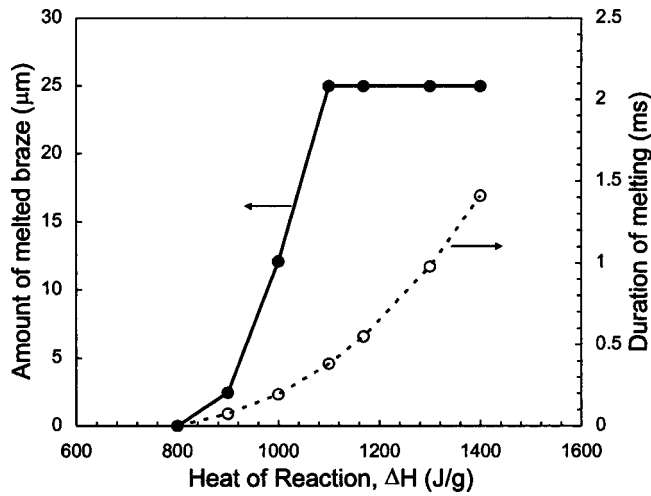


FIG. 10. Numerical parametric study which reflects the dependence of melting of the 25 μm predeposited braze layer on the heat of reaction ΔH of the Al/Ni reactive foil. The thickness of the foil and the velocity were kept constant at 100 μm and 5 m/s, respectively.

μm) before all the braze on the titanium melts and almost tripled (from 60 to 160 μm) before it is molten for 0.75 ms at the unbonded interface.

The effect of varying only the heat of reaction of the foils, while keeping the foil thickness constant at 100 μm and the velocity constant at 5 m/s is illustrated in Fig. 10. It is quite apparent that the melting of the braze is very sensitive to variations in the heat of reaction. A rise of just 25% in the heat of reaction of the foil increases the amount of braze that melts on the titanium component by ten times. Increasing the heat of reaction by 38% melts all the braze and increasing the heat of reaction by 55% keeps the braze molten for 0.75 ms at the unbonded interface. For comparison, one needs to increase the total foil thickness by 100% and 167% to achieve the same objectives. The heat of reaction has such a strong impact because it controls the temperature that the foils reach during reaction, as can be seen in Fig. 11. This has important consequences for heat flow as will be discussed.

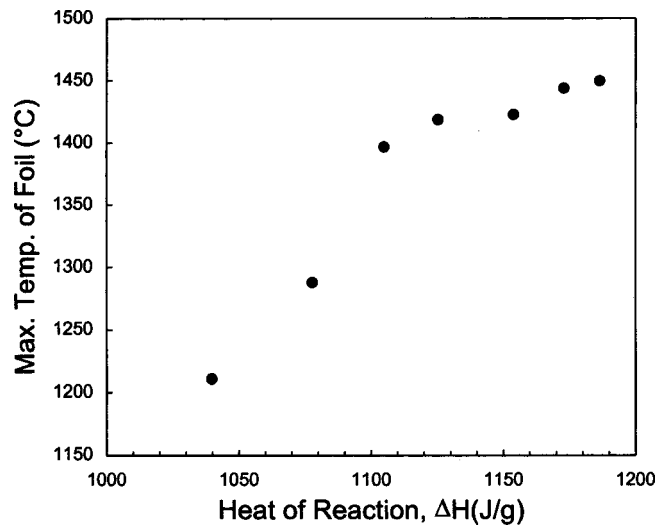


FIG. 11. The predicted maximum temperature reached in the reactive foil as a function of the measured heat of reaction.

IV. DISCUSSION

The upper strength limit of 35 MPa observed in this study seems on initial consideration to be surprising low if it is considered that the quoted yield strength of the braze used for joining is 338 MPa. However, when considering fracture this is easily understood. For the highest strength specimens, fracture always occurred in or along the CuTi interface layer between the braze and the titanium alloy component. This CuTi layer, which is presumably a brittle intermetallic layer, forms during the prebrazing process and not during the actual reactive joining process. Its fracture strength is likely to be low and is assumed to be limiting the measured shear strengths. Failure along this brittle interface layer is also likely to account for the fair amount of scatter observed in the maximum strength values (Fig. 5). As mentioned previously, another contributing factor to the low measured strengths is the mode of testing. Since the test specimens are single lap and are loaded in tension, there is a significant amount of nonshear loading which reduces the recorded shear strengths.

Regardless of the absolute joint strengths the trends observed in this study are very illuminating. For instance, it is clear that the measured joint strengths of this study do not depend critically on the total heat released by the reactive foils during joining, unlike in earlier studies involving lower melting point solder bonding layers.^{2,3} Note in Fig. 5(a) that a 4273 bilayer foil that is 160 μm thick results in a joint strength of 8 MPa. Assuming typical foil dimensions for the joint area it can be calculated that such a foil produces 101 J of total heat. However, a 2000 bilayer foil that is only 110 μm thick results in a much higher joint strength of 35 MPa, yet only produces 74 J of total heat. These experimental results can only be explained by considering the heat of reaction. Figs. 2 and 5(b) show that there is a clear dependency of both joint strength and heat of reaction on bilayer thickness, regardless of the number of bilayers. The thinner foil from the above example (110 μm thick), which resulted in a higher strength, has a bilayer thickness of 55 nm and a heat of reaction of 1164 J/g, while the thicker foil from the same example (160 μm thick), which has a smaller bilayer thickness of 37 nm and a smaller heat of reaction of 1036 J/g resulted in a lower joint strength. Figures 2 and 5(b) suggest that a heat of reaction equal to 1150 J/g (or a bilayer of 50 nm) is needed to achieve a strong joint in this particular geometry.

The modeling results of this study provide additional support for the above interpretation of the experimental results. When particular measured reactive foil properties are fed into the model, the predicted amount and time of braze melting do not demonstrate uniform dependencies on foil thickness, as seen in Fig. 7. Instead the data for the two sets of foils show separate trends and some thicker foils with more total heat are predicted to melt less braze for a shorter amount of time compared to other thinner foils with less total heat. The parametric studies also indicate that the success of braze melting is more sensitive to changes in the heat of reaction of the foils (Fig. 10) than changes in foil thickness or total heat (Fig. 9).

To understand why the success of melting a bonding layer with a high T_m , such as a braze, is critically dependent on the heat of reaction of the foil in reactive joining, one needs to consider the kinetic transfer of heat from the reactive foil to the braze layer. First, the braze material needs to absorb a sufficient quantity of heat to raise its temperature to its melting point and to cause melting. Second, this absorption of heat needs to occur rapidly, to minimize heat dissipation into the adjoining titanium component. The initial requirement is easily met (about 4 J of energy is required), but the second requirement depends on a number of factors, which include the relative temperatures, melting points, thermal conductivities, and heat capacities of the various layers involved. In this example, where a high melting point braze layer is involved, the difference between the maximum temperature of the reactive foil, T_{Fmax} , and the melting point of the braze, $T_{Brazemelt}$, is critical. The smaller this difference, the more difficult it will be to satisfy the second requirement. Alternatively, the higher T_{Fmax} , the more rapid the heat transfer into the braze layer and thus the more likely it will be to melt. The maximum temperature that the reactive foil reaches is in turn dependent on the heat of reaction of the foil, as can be seen in Fig. 11.

The importance of the temperature difference, $\Delta T = T_{Fmax} - T_{Brazemelt}$, can be used to explain the discrepancies between the modeling predictions and the experimental results. The modeling assumed that the braze melts at 715 °C, which is the published liquidus temperature for this commercial braze. However, due to the extensive Ti diffusion into the braze layer during the prebrazing process (prior to joining) the melting point of the braze was increased to 805 °C, as noted earlier. Since the modeling assumes a lower melting point for the braze, compared to that observed experimentally, the predictions are therefore less sensitive to the maximum foil temperatures. This explains why the separation of predicted data points for the two different reactive foil sets in Fig. 7 is smaller than the separation in Fig. 5(a) for the experimental results.

Lastly we consider the duration of melting and its influence on joint strength. When comparing the experimental strength results [Fig. 5(a)] with the predicted time of melting of the braze layer on the component (Fig. 7) for the reactive foil set consisting of 2000 bilayers, it was observed that the braze layers need to be molten at the braze/coated foil interface for a minimum time of about 0.75 ms to achieve maximum wetting and joint strength. This observation is consistent with an earlier study involving the reactive joining of stainless steel by melting a AuSn solder layer,³ where it was found that the AuSn solder needs to be molten for 0.5 ms in order to establish maximum joint strength. The reason for this minimum time of melting requirement for the bonding layer is likely related to the facilitation of flow of the molten material. If the bonding layer is molten for long enough it can flow to fill in any cracks or crevices and also expose fresh surfaces to enhance wetting. It is also interest-

ing to note that unlike the case for free-standing bonding layers (free-standing sheets of solder),^{2,3} complete melting of the braze layer that was pre-bonded to the component is not necessary for good joining results.

V. CONCLUSION

Titanium alloy components have been joined at room temperature by reactive joining: a process that harnesses the heat released by self-propagating exothermic reactions in multilayer foils to melt a silver-based braze. By systematically varying the properties of the reactive foil and by numerically modeling the reactive joining process for these conditions we were able to deduce that the maximum temperature reached by the foil during reaction was critical in determining the success of joining for this high melting point braze layer. The maximum temperature is directly dependent on the foil's heat of reaction. Other factors such as reaction velocity, foil thickness, and total heat have less impact on joint strength. Our current results also confirmed previous observations of highly refined solidification microstructures associated with reactive joining. They also confirm the notion that a minimum duration of melting of the bonding layer is necessary to ensure the success of the reactive joining process.

ACKNOWLEDGMENT

This work was supported by the National Science Foundation through Grant No. DMI-0115238.

¹D. M. Makowiecki and R. M. Bionta, US Patent No. 5381944 (17 January 1995).

²J. Wang *et al.*, Appl. Phys. Lett. **83**, 3987 (2003).

³J. Wang, E. Besnoin, A. Duckham, S. J. Spey, M. E. Reiss, O. M. Knio, and T. P. Weihs, J. Appl. Phys. **95**, 248 (2004).

⁴S. J. Spey, E. Besnoin, A. Duckham, M. E. Reiss, J. Wang, O. M. Knio, and T. P. Weihs, J. Am. Ceram. Soc. (submitted).

⁵T. P. Weihs, T. C. Hufnagel, O. M. Knio, M. E. Reiss, D. V. Heerden, and H. Feldmesser, US Patent Appl. No. 20020182436 (18 April 2002).

⁶A. J. Swiston, T. C. Hufnagel, and T. P. Weihs, Scr. Mater. **48**, 1575 (2003).

⁷E. Besnoin, O. M. Knio, J. Wang, A. Duckham, S. J. Spey, D. V. Heerden, and T. P. Weihs, Provisional US Patent (13 May 2003).

⁸A. Mann, A. Gavens, M. E. Reiss, D. V. Heerden, G. Bao, and T. P. Weihs, J. Appl. Phys. **82**, 1178 (1997).

⁹T. W. Barbee and T. P. Weihs, US Patent No. 5547715 (20 August 1996).

¹⁰M. E. Reiss, C. M. Esber, D. V. Heerden, A. J. Gavens, M. E. Williams, and T. P. Weihs, Mater. Sci. Eng., A **261**, 217 (1999).

¹¹A. J. Gavens, D. V. Heerden, A. B. Mann, M. E. Reiss, and T. P. Weihs, J. Appl. Phys. **87**, 1255 (2000).

¹²S. Jayaraman, A. B. Mann, T. P. Weihs, and O. M. Knio, 27th Symposium (International) on Combustion, 1998 (The Combustion Institute, Pittsburgh, PA, 1998), p. 2459

¹³S. Jayaraman, O. M. Knio, A. B. Mann, and T. P. Weihs, J. Appl. Phys. **86**, 800 (1999).

¹⁴S. Jayaraman, A. B. Mann, M. E. Reiss, T. P. Weihs, and O. M. Knio, Combust. Flame **124**, 178 (2001).

¹⁵E. Besnoin, S. Cerutti, O. M. Knio, and T. P. Weihs, J. Appl. Phys. **92**, 5474 (2002).

¹⁶L. A. Clevenger, C. V. Thompson, and K. N. Tu, J. Appl. Phys. **67**, 28 (1990).

¹⁷T. S. Dyer, Z. A. Munir, and V. Ruth, Scr. Metall. Mater. **30**, 1281 (1994).

¹⁸T. P. Weihs, in *Handbook of Thin Film Process Technology*, edited by D. A. Glocker and S. I. Shan (IOP Publishing, London, 1998).